Ecological Research

WILEY

TECHNICAL NOTE OPEN ACCESS

Genetic Diversity in the Wrinkled Frog, *Glandirana rugosa*, Evaluated Using Microsatellite Markers Identified by Nanopore Sequencing

Yuzuna Fukatsu[1] | Takeshi Igawa[2] | Kaito Sasaki[1] | Satoshi Yamagishi[1] | Teruhiko Takahara[1,3,4]

[1]Graduate School of Life and Environmental Sciences, Shimane University, Matsue, Shimane, Japan | [2]Amphibian Research Center, Hiroshima University, Hiroshima, Hiroshima, Japan | [3]Faculty of Life and Environmental Sciences, Shimane University, Matsue, Shimane, Japan | [4]Estuary Research Center, Shimane University, Matsue, Shimane, Japan

Correspondence: Takeshi Igawa (tigawa@hiroshima-u.ac.jp) | Teruhiko Takahara (ttakahara@life.shimane-u.ac.jp)

Received: 7 March 2025 | **Revised:** 12 August 2025 | **Accepted:** 11 September 2025

Funding: This work was supported by Oki Islands UNESCO Global Geopark.

Keywords: amphibian | cryptic species | genetic diversity | population genetics | simple sequence repeat

ABSTRACT

Wrinkled frogs (*Glandirana rugosa*) are a common species found in various freshwater habitats across Japan. Due to multiple sex chromosome turnovers and the discovery of cryptic species, understanding the historical population dynamics of this species is crucial for studying its genomic evolution and speciation. On the other hand, in some populations, urbanization has led to a decline in both population size and their distribution range. To better understand the historical population dynamics and recent population decline of *G. rugosa*, it can be helpful to conduct novel genetic analyses. As a crucial first step, we primarily focused on developing 14 microsatellite markers using nanopore sequencing. These markers were then validated by assessing the genetic diversity of *G. rugosa* in four populations: three from mainland Japan (two from Shimane and one from Gunma Prefectures) and one from an island (Oki Islands, Shimane Prefecture). The total number of alleles per locus ranged from 4 to 36, and the observed heterozygosity ranged from 0 to 0.950. Population genetic analyses using these markers revealed substantial genetic diversity among populations and a weak correlation between intra-population diversity and geographical features. We believe that the microsatellite markers developed in this study would be useful in exploring their genetic diversity in other populations and contribute to the conservation of this species in the future.

1 | Introduction

The analysis of population dynamics using genetic markers is crucial for understanding speciation and population diversification. Genetic diversity, which reflects both historical and ongoing population processes, is a key factor in demonstrating evolutionary plasticity. It is also critical for the long-term stability and resilience of populations. Studying species with diverse genetic backgrounds can help advance our understanding of both evolutionary processes and conservation efforts (Frankham 2005).

The wrinkled frog (*Glandirana rugosa*) is a common anuran amphibian that is widely distributed across Honshu (mainland Japan), Shikoku, Kyushu, and Hokkaido (artificial distribution), inhabiting a variety of environments, such as paddy fields, ponds, and rivers. This species is unique because it encompasses multiple populations with distinct sex determination systems (XY and ZW) within the same species (Miura 2008). Recent studies have further revealed cryptic diversity within *G. rugosa*. Two local populations have been described as new species: *Glandirana susurra* from Sado Island, identified based on morphological traits and mitochondrial DNA divergence using

genetic analyses (Sekiya et al. 2012), and *Glandirana reliquia* from the Pacific Ocean side of the Kanto and Tohoku regions, distinguished by morphological features and analyses of both mitochondrial and nuclear DNA (Shimada et al. 2022). These findings show the importance of reconstructing the historical population dynamics of *G. rugosa* to elucidate its genomic evolution and speciation processes. Also, although *G. rugosa* is generally considered a common species, habitat loss and fragmentation caused by urbanization, particularly in Tokyo and Gunma Prefectures in the Kanto region, where it is listed as endangered (Fukuyama and Kusano 2023; Kanai 2022), have resulted in a decline in both population size and its distribution range. To better understand the historical population dynamics and recent population decline of *G. rugosa*, it can be helpful to conduct novel genetic analyses.

Microsatellites are regions of genomic DNA composed of repeating sequences, typically two–five nucleotides per repeat unit. The number of repeats can vary at the individual level. Due to the relatively low sampling labor and experimental costs, population genetic analysis using microsatellite polymorphisms remains the preferred method for molecular, ecological, and conservation genetic studies of amphibians (Igawa et al. 2011, 2020; Komaki et al. 2014). Moreover, recent advancements in long-read sequencing technologies have facilitated the identification of these long repetitive regions (Asaeda et al. 2023).

In this study, as a crucial first step, we primarily focused on developing microsatellite markers for *G. rugosa* using the Oxford Nanopore sequencer (Oxford Nanopore Technologies, Oxford, UK) and evaluated the usefulness of these markers for assessing the genetic diversity of this species. We examined the intra- and inter-population genetic diversity of four *G. rugosa* populations with different geographic distances and environments in Japan: three from Shimane Prefecture (two on the mainland and one on Dogo Island within the Oki Islands), where the species is classified as common, and a high-altitude population near a lake in Gunma Prefecture.

2 | Methods

2.1 | Study Sites

We collected frogs from four locations: Honjo (HON), Aika (AIK), and Oki Islands (OKI) in Shimane Prefecture, and one site in Gunma (GUN) Prefecture in Japan (Figure 1; Table S1a). HON is a rice paddy used for field experiments managed by Shimane University and is surrounded by small waterways, reservoirs, and mountains. AIK comprises rice fields bordered by small rivers and mountains. OKI is situated near a mountain stream on Dogo Island, the Oki Islands, Shimane Prefecture, and coexists sympatrically with *Rana okiensis* and *Hynobius okiensis*, which are both endemic to the Oki Islands. GUN is located around Kono Pond, a crater lake on Mt. Akagi, approximately 1400 m above sea level, and is surrounded by forests.

From 2021 to 2022, we collected a total of 106 *G. rugosa* individuals: 29 from HON, 31 from AIK, 24 from OKI, and 22 from GUN. The collected frogs were anesthetized using a 1% solution of tricaine methane sulfonate (MS-222). The distal extremities

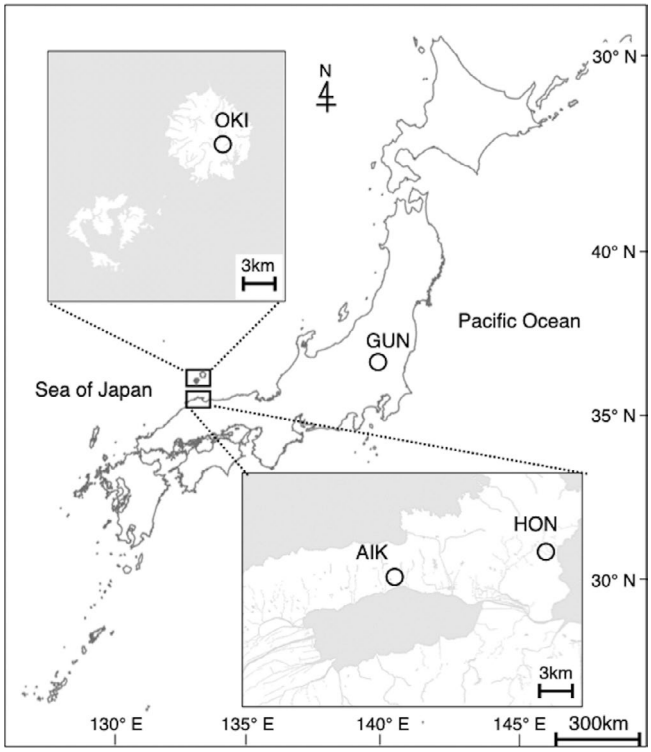

FIGURE 1 | Location information for the four populations in Japan (HON, AIK, OKI, and GUN). The maps are based on the Digital Map (Basic Geospatial Information) published by the Geospatial Information Authority of Japan (http://maps.gsi.go.jp/). Honjo (HON), Aika (AIK), and Oki Islands (OKI) in Shimane Prefecture; Gunma (GUN) Prefecture.

of the hind limbs were then amputated, and the samples were preserved in 70% ethanol. The frogs were returned to their respective collection sites after the procedure.

2.2 | DNA Extraction

DNA was extracted from the hind limb distal extremities of *G. rugosa* using a DNeasy Blood & Tissue kit (Qiagen, Hilden, Germany), according to the manufacturer's instructions. For DNA extraction, 100 μL of buffer AE was added, and the DNA concentrations were measured using fluorescence quantification equipment (NanoDrop Lite; Thermo Fisher Scientific, Carlsbad, CA, USA). The samples were stored in a freezer until subsequent experiments.

2.3 | Genome Sequencing and Development of Microsatellite Markers

The extracted genomic DNA in OKI (Table S1b) was used for library construction using a ligation library preparation kit (SQK-LSK110; Oxford Nanopore Technologies, Oxford, UK). Following the manufacturer's instructions, the quality and molecular weight of the genomic DNA were assessed using a Qubit (Thermo Fisher Scientific). Sequencing was performed using a MinION sequencer (MinION Mk1B; Oxford Nanopore Technologies) with a Flongle flow cell (FLO-FLG001; Oxford Nanopore Technologies). Base-called sequence reads were

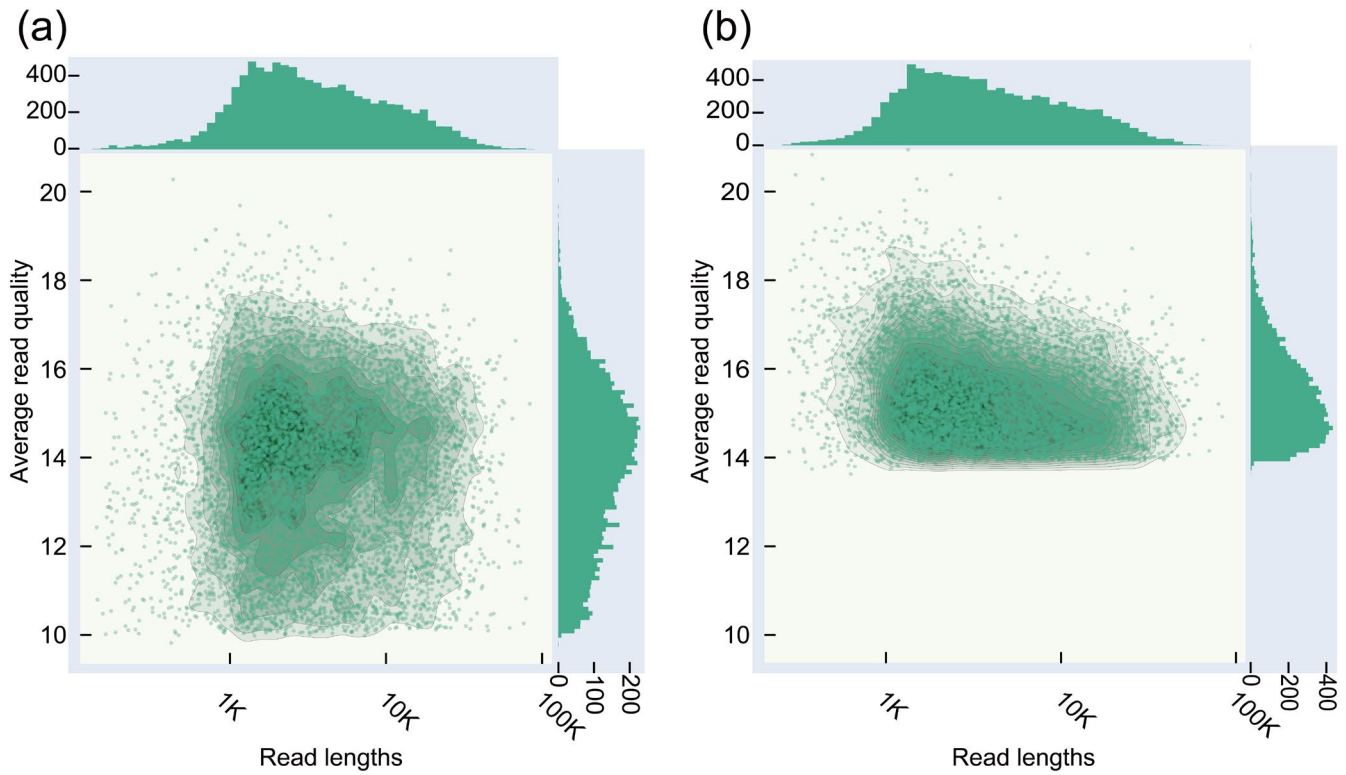

FIGURE 2 | Bivariate plot of log-transformed read length against average read quality plot for (a) raw and (b) filtered nanopore sequence data.

obtained using the super-accurate, base-calling models in MinKNOW (version 21.06.13) and Guppy (version 5.0.16). The first 75 bases of each read were trimmed, and reads shorter than 300 bases or with an average quality score below 14 were excluded from the microsatellite primer design using NanoFilt (De Coster et al. 2018). Microsatellite primers were designed using msatcommander (Faircloth 2008) to amplify loci containing microsatellite regions with two–four base repeats of 10–30 repetitions. These primers were validated using the genome sequence data from *G. rugosa* (Katsura et al. 2021) and electronic polymerase chain reaction using the Reverse e-PCR search cmdline tool version 2.3.9 (Schuler 1997). The primers that amplified a single locus were selected, resulting in 104 primer pairs. Amplification and polymorphism of these primer pairs were tested using four DNA samples from three locations in Shimane Prefecture (Kashima Town, Taki Town, and OKI) (Table S1b). We identified polymorphic loci by detecting distinct size peaks (alleles). For multiplexed and multicolored genotyping (Shimizu and Yano 2011), barcoded slit tags (BStag) were added to primer pairs that were successfully amplified and showed polymorphisms. The combination of BStag primers and fluorescent dyes was performed as previously described (Igawa et al. 2015).

2.4 | Microsatellite Polymorphism Analysis

We investigated 14 microsatellite loci, which were amplified in electronic and virtual PCR and polymorphic in the pilot experiments (see Results). The combination of primers and fluorescent dyes followed the protocol described previously (Igawa et al. 2015). The loci were amplified using PCR with KOD FX Neo (TOYOBO Co. Ltd., Osaka, Japan). The reaction mixture consisted of 0.5 μL of genomic DNA (diluted 1:2), 0.2 μL of KOD FX Neo, 4.8 μL of buffer, 1.6 μL of 2.0 mM dNTP mix, 0.05 μL of 10 μM tagged primer, 0.1 μL of 20 μM untagged primer, and 0.05 μL of 10 μM fluorescent dye-labeled primer. The PCR cycling conditions were: 95°C for 3 min, followed by 30 cycles of 98°C for 10 s, 58°C for 30 s, and 68°C for 30 s. The final eight cycles were performed with the following conditions: 98°C for 10 s, 49°C for 30 s, and 68°C for 30 s.

The amplified fragments were subjected to electrophoresis using an ABI 3130xl Genetic Analyzer (Thermo Fisher Scientific). The fragment size and genotype of the loci were determined using GeneMapper and GeneScan 500 Liz (Thermo Fisher Scientific) as an internal size standard.

2.5 | Population Genetic Analyses

The number of alleles (N_A), observed heterozygosity (H_O), expected heterozygosity (H_E), inbreeding coefficient (F), and genetic distance between populations (F_{ST}) were calculated using GenAlEx 6.5 (Peakall and Smouse 2012). Deviations from the Hardy–Weinberg equilibrium (HWE) and linkage disequilibrium of the genotypes were assessed using GENEPOP4.7.5 (Rouset 2008), with Bonferroni correction applied for multiple testing. Nei et al.'s D_A distances (D_A) between populations were calculated, and phylogenetic trees based on F_{ST} and D_A were constructed using POPTREE2 (Takezaki et al. 2010). Bootstrap values of the trees were calculated using 1000 iterations. Isolation by distance (IBD) (correlation of genetic (F_{ST}) and geographic distance) was checked using the "mantel" function in GenAlEx 6.5. For the calculation of population genetic indexes of GUN and genetic distance analyses, including GUN, we used nine loci, excluding five loci that could not be amplified in GUN.

TABLE 1 | Characterization of 14 microsatellite loci isolated from *Glandirana rugosa*.

No.	Loci	Accession no.	Repeat motif	Primer sequence (5′-3′)	Dye	Size ranges (bp)	Multiplex
1	*Grugo1128*	LC884696	$(AC)_{11}$	F: *F9CCG*-TGACCACCTTGCTCGTGTAC	FAM	280–330	I
				R: AACCTCTCTCAGCAACCACC			
2	*Grugo4579*	LC884697	$(AT)_{14}$	F: *F9CCG*-GAGCCAGAACAGGAAACCAC	FAM	220–330	II
				R: AGGGCCCTTTGATTCTCTCC			
3	*Grugo7057*	LC884698	$(AT)_{26}$	F: AGTGCTCCAGACCATACACC	HEX	200–370	II
				R: *F9GTC*-TAGTGGCCTGGGATTGTCTG			
4	*Grugo12056*	LC884699	$(AT)_{11}$	F: TGGATCGGCAGGTCTACATC	NED	280–330	II
				R: *F9TAC*-ATTAAGCCACGCCTCTGTCC			
5	*Grugo17393*	LC884700	$(AC)_{28}$	F: TGATGGAGGAGTGGAAGAGC	FAM	360–480	III
				R: *F9GAC*-TCAACCAAGCCTCTGGAACC			
6	*Grugo8343*	LC884701	$(AT)_{23}$	F: *F9AGG*-GCCGTCACCAATGCTTGTAG	HEX	340–410	III
				R: CCTTTCATGGGCAATCGGAG			
7	*Grugo13863*	LC884702	$(AT)_{20}$	F: TGGCGTATGACTACTGGACC	FAM	400–450	IV
				R: *F9GAC*-GCTACTATGCACAGGGAAGAG			
8	*Grugo15278*	LC884703	$(AC)_{28}$	F: *F9GTC*-TATCACCATTGGAGGCCCTG	HEX	360–520	V
				R: GCCCAATCTTCAAGCCCATC			
9	*Grugo12007*	LC884704	$(AGAT)_{16}$	F: *F9GAC*-AGAGCGGCATAAGAGGACTG	FAM	380–550	VI
				R: AGCCACTGACCAAGGATGAG			
10	*Grugo17120*	LC884705	$(AT)_{26}$	F: *F9AGG*-GCCAATGAACACACCAAGAC	HEX	320–380	VI
				R: TGGCGGACAGGACATAGTTC			
11	*Grugo11308*	LC884706	$(AC)_{12}$	F: GGTTTAAGTGCCCAGTGGTC	FAM	430–470	VII
				R: *F9GAC*-AAGCCACCTCAACCCAGTAG			
12	*Grugo13811*	LC884707	$(AC)_{19}$	F: TTGGCCGAAACCTGAATTGG	FAM	170–210	VIII
				R: *F9CCG*-TCTCTGACCAAATAAGCGGC			
13	*Grugo16767*	LC884708	$(AT)_{12}$	F: TGGCTAGCAGTGGAGTCATC	FAM	420–530	VIII
				R: *F9GAC*-ATTGCACCTCACACACCATG			
14	*Grugo15644*	LC884709	$(AT)_{18}$	F: CGTGCTCTGTGTGAAAGGAG	FAM	290–330	IX
				R: *F9CCG*-TTGCAATTATGTGACCGCCG			

3 | Results

The total sequenced nucleotides of the *G. rugosa* using the ONT MinION/Flongle was 195,325,793 bp (Table S2) (total reads: 30,226; read length N50: 12,574 bp; average read length: 6462 bp; median read quality: 14.0; Figure 2a). After trimming, the dataset was reduced to 98,199,878 bp (Table S2) (total reads: 15,189; read length N50: 12,349 bp; average read length: 6465 bp; median read quality: 15.4; Figure 2b). We identified 19,282 repeat sequences in 5976 reads and designed 6404 primer sets. Data were deposited in the DDBJ Sequence Read Archive (DRA) under accession number DRR707529.

After verifying single locus amplification using electronic PCR and confirming polymorphism through virtual PCR, we identified 14 polymorphic microsatellite markers (Table S2). After Bonferroni correction, no significant linkage disequilibrium occurred between any of the loci, and *Grugo1128*, *Grugo17393*, *Grugo15278*, and *Grugo12007* showed significant deviation from HWE ($p < 0.00028$). The characteristics of the 14 loci are summarized in Table 1. Of these loci, amplification of five loci failed in GUN (Table 2). In summary, *Grugo12007* exhibited the highest number of polymorphisms, with a total of 36 alleles and an expected heterozygosity (H_E) of more than 0.8 in each population, whereas *Grugo15644* showed the lowest level of polymorphisms, with only four alleles and a H_E of less than 0.142 in the three populations in Shimane Prefecture. Of the four populations, HON and AIK exhibited the highest intrapopulation genetic diversity. The genetic distances between the populations (D_A and F_{ST}) based on the nine commonly genotyped loci are presented in Table 3. The highest genetic distance was observed between the three populations in Shimane Prefecture (HON, AIK, and OKI) and GUN, with a mean D_A of 0.840 and a mean F_{ST} of 0.375. Within Shimane Prefecture, OKI showed

TABLE 2 | Number of alleles and heterozygosities of 14 microsatellite loci in four populations [Honjo (HON), Aika (AIK), and Oki Islands (OKI) in Shimane Prefecture; Gunma (GUN) Prefecture].

		All sites		HON ($N=29$)			AIK ($N=31$)			OKI ($N=24$)			GUN ($N=22$)		
No.	**Loci**	N_A	F_{ST}	N_A	H_O	H_E	N_A	H_O	H_E	N_A	H_O	H_E	N_A	H_O	H_E
1	*Grugo1128*	16	0.306	9	0.793	0.785	**11**	**0.516**	**0.850**	3	0.583	0.556	3	0.063	0.174
2	*Grugo4579*	16	0.546	5	0.273	0.640	13	0.476	0.890	2	0.000	0.100			
3	*Grugo7057*	17	0.213	9	0.857	0.832	10	0.567	0.880	4	0.909	0.635	5	0.333	0.491
4	*Grugo12056*	19	0.278	7	0.586	0.543	15	0.862	0.898	3	0.409	0.625	6	0.429	0.524
5	*Grugo17393*	34	0.096	**12**	**0.793**	**0.845**	18	0.833	0.891	9	0.917	0.863	12	0.950	0.853
6	*Grugo8343*	24	0.144	16	0.897	0.857	15	0.897	0.887	6	0.542	0.806	3	0.600	0.649
7	*Grugo13863*	13	0.293	10	0.690	0.777	8	0.440	0.738	6	0.375	0.761	3	0.182	0.169
8	*Grugo15278*	28	0.109	10	0.714	0.803	**14**	**0.444**	**0.909**	9	0.708	0.740	9	0.864	0.825
9	*Grugo12007*	36	0.093	15	0.897	0.879	17	0.929	0.913	11	0.875	0.863	**11**	**0.467**	**0.800**
10	*Grugo17120*	14	0.436	6	0.586	0.748	11	0.464	0.794	4	0.583	0.540			
11	*Grugo11308*	12	0.451	5	0.333	0.632	9	0.370	0.837	3	0.222	0.545			
12	*Grugo13811*	15	0.462	6	0.357	0.660	12	0.385	0.857	2	0.500	0.375			
13	*Grugo16767*	26	0.179	9	0.538	0.800	14	0.793	0.779	4	0.333	0.527	8	0.619	0.747
14	*Grugo15644*	4	0.927	3	0.069	0.067	2	0.077	0.142	1	0.000	0.000			
	Mean	19.571	0.324	8.714	0.599	0.705	12.071	0.575	0.805	4.786	0.497	0.567	6.667	0.501	0.581

Note: N_A: number of alleles, F_{ST}: genetic distance between populations, H_O and H_E: observed and expected heterozygosity (values significantly different from Hardy–Weinberg equilibrium (HWE) are in bold).

TABLE 3 | Pairwise distances (F_{ST} and D_A) between each population of *Glandirana rugosa* (Honjo (HON), Aika (AIK), and Oki Islands (OKI) in Shimane Prefecture; Gunma (GUN) Prefecture). Below diagonal: F_{ST}, above diagonal: D_A (calculated based on nine loci excluding four null loci in GUN).

	HON	AIK	OKI	GUN
HON	—	0.516	0.722	0.838
AIK	0.062	—	0.629	0.797
OKI	0.231	0.187	—	0.884
GUN	0.363	0.328	0.433	—

Note: F_{ST}: fixation index, D_A: Nei's D_A genetic distance.

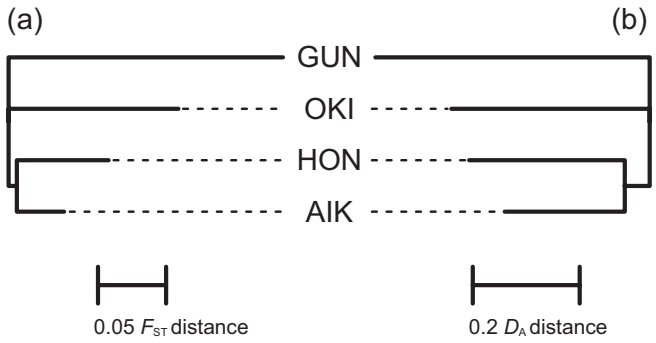

FIGURE 3 | Phylogenetic relationships among the four populations of *Glandirana rugosa* (a) Inferred from pairwise distance (F_{ST}), and (b) pairwise distance (D_A). Honjo (HON), Aika (AIK), and Oki Islands (OKI) in Shimane Prefecture; Gunma (GUN) Prefecture.

the greatest divergence. IBD analysis showed a positive correlation between genetic (F_{ST}) and geographic distances, with an R^2 value of 0.750 (Mantel correlation coefficient, Rxy = −0.557, $p = 0.04$). The phylogenetic tree based on F_{ST} and D_A distances also reflected these IBD relationships (Figure 3a,b).

4 | Discussion

We successfully developed highly polymorphic microsatellite markers for *G. rugosa* using the Flongle flow-cell, a cost-effective method for nanopore sequencing. The accuracy of the SQK-LSK110 sequencing kit was sufficient for designing primers to amplify the loci. The success rate of marker development (i.e., the number of developed markers versus the number of primer sets examined) was 13.4%. This ratio was lower than that reported in previous studies using IonPGM [23.5% for *Odorrana narina* (Igawa et al. 2015), 20.0% for *Buergeria japonica* (Komaki et al. 2014) and 25.0% for *Hynobius retardatus* (Matsunami et al. 2015)] but sufficiently efficient when considering its ease and rapid benchtop sequencing at a lower cost (Approximately 2000 USD, including a Flongle flow cell and reagents for library construction).

The mean expected heterozygosity (H_E) of *G. rugosa* in the four populations (0.567–0.805) was higher than that of the endangered Japanese frogs *Odorrana ishikawae* and *Odorrana splendida* (0.358 and 0.439, respectively) (Igawa et al. 2013) and similar to that of the congenic species, *Glandirana emeljanovi* (formerly *Rana emeljanovi*) in Korea (0.816) (Kim et al. 2016). Therefore, the high genetic diversity of *G. rugosa* was expected to be maintained in all four populations examined in the current study. Within the four populations, OKI and GUN exhibited slightly lower H_E values (0.567 and 0.581, respectively). *Glandirana rugosa* is usually found in a variety of habitats but is believed to be primarily found in plain fields (Matsusi and Maeda 2018). As OKI is an island population and GUN is located in a mountainous area at an altitude of approximately 1400 m, the lower H_E values may reflect their smaller distribution areas and smaller population sizes. Therefore, genetic data derived from the newly developed microsatellite markers are useful for inferring the genetic diversity and demographic characteristics of *G. rugosa* populations.

Genetic distances (D_A and F_{ST}) among the four populations were associated with their geographic distances. A genetic distance was detected between HON and AIK, which were approximately 15 km apart (0.516 in D_A and 0.062 in F_{ST}). This may be due to the presence of several low ridges and rivers separating HON and AIK. Therefore, the resolution of these markers should be sufficiently high to detect migration rates and identify individual kinships among local populations. As the sex chromosomes of Western and Eastern Japanese populations of *G. rugosa* are different (both XY sex chromosomes but different origins; Miura 2008), there should be a structural difference in the genome between GUN (Eastern Japan) and other populations (Western Japan). This may be the reason why the number of available loci is limited in GUN, but even the nine loci seemed to be sufficient to examine population dynamics.

Recently, several new species and populations with different sex chromosomes have been identified within this species (Miura 2008, 2013; Shimada et al. 2022), likely resulting from migration and geographic isolation among populations. Therefore, it is important to investigate the ongoing migration of these new species and genetically distinct populations. In addition, populations showing considerable genetic variation may indicate the presence of cryptic species, so we analyzed one population from the Kanto region (within the range of *G. reliquia*) and another from the Oki Islands, referencing *G. susurra* from Sado Island. Although this study did not detect clear genetic differences among these populations, considering the geographic barrier and distance, applying our markers to additional populations in future studies may help uncover hidden genetic structure and potentially reveal new species. The microsatellite markers developed in this study will be useful for research focusing on these intrinsic population dynamics and for conservation management of *G. rugosa*.

Acknowledgments

This study was supported by the Oki Islands UNESCO Global Geopark in 2021. We sincerely thank the Department of Molecular and Functional Genomics, Interdisciplinary Center for Science Research, Organization for Research and Academic Information, Shimane University, Japan, for providing the Genetic Analyzer. The authors thank the SDGs Research Project and the Faculty of Life and Environmental Sciences at Shimane University, Japan, for their financial support in publishing this report. The survey and all the experiments were conducted in compliance with Japan's current laws.

Conflicts of Interest

The authors declare no conflicts of interest.

References

Asaeda, Y., K. Shiraga, M. Suzuki, Y. Sambongi, H. Ogino, and T. Igawa. 2023. "Rapid and Collective Determination of the Complete "Hot-Spring Frog" Mitochondrial Genome Containing Long Repeat Regions Using Nanopore Sequencing." *PLoS One* 18: e0280090. https://doi.org/10.1371/journal.pone.0280090.

De Coster, W., S. D'hert, D. T. Schultz, M. Cruts, and C. Van Broeckhoven. 2018. "NanoPack: Visualizing and Processing Long-Read Sequencing Data." *Bioinformatics* 34: 2666–2669. https://doi.org/10.1093/bioinformatics/bty149.

Faircloth, B. C. 2008. "MSATCOMMANDER: Detection of Microsatellite Repeat Arrays and Automated, Locus-Specific Primer Design." *Molecular Ecology Resources* 8: 92–94. https://doi.org/10.1111/j.1471-8286.2007.01884.x.

Frankham, R. 2005. "Genetics and Extinction." *Biological Conservation* 126: 131–140. https://doi.org/10.1016/j.biocon.2005.05.002.

Fukuyama, K., and T. Kusano. 2023. "Wrinkled Frog Glandirana rugosa." In *Red Data Book Tokyo 2023: 23-Ward and Tama Area Version*, edited by The Natural Environment Division, Bureau of Environment, Tokyo Metropolitan Government, 523. Kowa Product Co., Ltd.

Igawa, T., M. Nozawa, M. Nagaoka, et al. 2015. "Microsatellite Marker Development by Multiplex Ion Torrent PGM Sequencing: A Case Study of the Endangered *Odorrana narina* Complex of Frogs." *Journal of Heredity* 106: 131–137. https://doi.org/10.1093/jhered/esu071.

Igawa, T., M. Okuda, S. Oumi, et al. 2011. "Isolation and Characterization of Twelve Microsatellite Loci of Endangered Ishikawa's Frog (*Odorrana ishikawae*)." *Conservation Genetics Resources* 3: 421–424. https://doi.org/10.1007/s12686-010-9370-7.

Igawa, T., S. Oumi, S. Katsure, and M. Sumida. 2013. "Population Structure and Landscape Genetics of Two Endangered Frog Species of Genus *Odorrana*: Different Scenarios on Two Islands." *Heredity* 110: 46–56. https://doi.org/10.1038/hdy.2012.59.

Igawa, T., H. Sugawara, M. Honda, et al. 2020. "Detecting Inter and Intraisland Genetic Diversity: Population Structure of the Endangered Crocodile Newt, *Echinotriton andersoni*, in the Ryukyus." *Conservation Genetics* 21: 13–26. https://doi.org/10.1007/s10592-019-01219-8.

Kanai, K. 2022. "Wrinkled Frog *Glandirana rugosa*. In The Natural Environment Division, Gunma Prefecture Government." In *Red Data Book Gunma 2022: Animals*, 97. Journal Print. Co., Ltd.

Katsura, Y., T. Ikemura, R. Kajitani, et al. 2021. "Comparative Genomics of *Glandirana Rugosa* Using Unsupervised AI Reveals a High CG Frequency." *Life Science Alliance* 4: e202000905. https://doi.org/10.26508/lsa.202000905.

Kim, D. Y., D. Kim, S. K. Park, H. Lee, H. Y. Suk, and M. S. Min. 2016. "Isolation and Characterization of Novel Microsatellite Loci in the Wrinkled Frog." *Genetics and Molecular Research* 15: gmr.15017183. https://doi.org/10.4238/gmr.15017183.

Komaki, S., T. Igawa, M. Nozawa, S.-M. Lin, S. Oumi, and M. Sumida. 2014. "Development and Characterization of 14 Microsatellite Markers for *Buergeria Japonica* (Amphibia, Anura, Rhacophorida)." *Genes & Genetic Systems* 89: 35–39. https://doi.org/10.1266/ggs.89.35.

Matsunami, M., T. Igawa, M. Nozawa, H. Michimae, T. Miura, and K. Nishimura. 2015. "Development and Characterization of 12 Microsatellite Markers for the Hokkaido Salamander (*Hynobius retardatus*)." *Current Herpetology* 34: 177–181. https://doi.org/10.5358/hsj.34.177.

Matsusi, M., and N. Maeda. 2018. *Encyclopaedia of Japanese Frogs*. Bunichi Sogo Shuppan.

Miura, I. 2008. "An Evolutionary Witness: The Frog, *Rana Rugosa*, Underwent Change of Heterogametic Sex From XY Male to ZW Female." *Sexual Development* 1: 323–331. https://doi.org/10.1159/000111764.

Miura, I. 2013. "*Glandirana Susura* as New Species—Mystery of Its Birth and Evolution." *Biotechnology* 91: 161–164.

Peakall, R., and P. E. Smouse. 2012. "GenAlEx 6.5: Genetic Analysis in Excel. Population Genetic Software for Teaching and Research—An Update." *Bioinformatics* 28: 2537–2539. https://doi.org/10.1093/bioinformatics/bts460.

Rouset, F. 2008. "GENEPOP'007: A Complete Re-Implementation of the GENEPOP Software for Windows and Linux." *Molecular Ecology Resources* 8: 103–106. https://doi.org/10.1111/j.1471-8286.2007.01931.x.

Schuler, G. D. 1997. "Sequence Mapping by Electronic PCR." *Genome Research* 7: 541–550. https://doi.org/10.1101/gr.7.5.541.

Sekiya, K., I. Miura, and M. Ogata. 2012. "A New Frog Species of the Genus *Rugosa* From Sado Island, Japan (Anura, Ranidae)." *Zootaxa* 3573: 49–62. https://doi.org/10.11646/zootaxa.3575.1.3.

Shimada, T., M. Matsui, M. Ogata, et al. 2022. "Genetic and Morphological Variation Analyses of *Glandirana rugosa* With Description of a New Species (Anura, Ranidae)." *Zootaxa* 5174: 25–45. https://doi.org/10.11646/ZOOTAXA.5174.1.2.

Shimizu, T., and K. Yano. 2011. "A Post-Labeling Method for Multiplexed and Multicolored Genotyping Analysis of SSR, Indel and SNP Markers in Single Tube With Bar-Coded Split Tag (BStag)." *BMC Research Notes* 4: 1–9. https://doi.org/10.1186/1756-0500-4-161.

Takezaki, N., M. Nei, and K. Tamura. 2010. "POPTREE2: Software for Constructing Population Trees From Allele Frequency Data and Computing Other Population Statistics With Windows Interface." *Molecular Biology and Evolution* 27: 747–752. https://doi.org/10.1093/molbev/msp312.

Supporting Information

Additional supporting information can be found online in the Supporting Information section. **Table S1:** Information of each sampling site. **Table S2:** Summary of microsatellite development efficiency based on nanopore sequencing.